MEDICAL SCIENCE MONITOR

DIAGNOSTIC TECHNIQUES

e-ISSN 1643-3750
© Med Sci Monit, 2019; 25: 341-356
DOI: 10.12659/MSM.913396

Received: 2018.09.28
Accepted: 2018.12.27
Published: 2019.01.11

The Role of Disturbed Small-World Networks in Patients with White Matter Lesions and Cognitive Impairment Revealed by Resting State Function Magnetic Resonance Images (rs-fMRI)

Authors' Contribution:
Study Design A
Data Collection B
Statistical Analysis C
Data Interpretation D
Manuscript Preparation E
Literature Search F
Funds Collection G

BCDEF 1,2 Jinfang Wang
E 3 Yu Chen
B 4 Huazheng Liang
B 4 Garry Niedermayer
B 5 Hongyan Chen
B 1 Yuexiu Li
C 1 Meiru Wu
ACG 1 Yongjun Wang
ADEG 1 Yumei Zhang

1 Department of Neurology, Beijing Tiantan Hospital, Capital Medical University; China National Clinical Research Center for Neurological Diseases; Center of Stroke, Beijing Institute for Brain Disorders; Beijing Key Laboratory of Translational Medicine for Cerebrovascular Disease, Beijing, P.R. China
2 Department of Neurology, General Hospital of The Yang Tze River Shipping, Wuhan Brain Hospital, Wuhan, Hubei, P.R China
3 School of Psychology, Brain and Mind Centre, University of Sydney; Australian Research Council Centre of Excellence in Cognition and Its Disorders, Sydney, NSW, Australia
4 School of Medicine, Western Sydney University, Campbelltown, NSW, Australia
5 Department of Radiology, Beijing Tiantan Hospital, Capital Medical University, Beijing, P.R. China

Corresponding Author: Yumei Zhang, e-mail: zhangyumei95@aliyun.com, meini96@sohu.com

Source of support: This work was funded by Beijing Municipal Administration of Hospitals Clinical Medicine Development of Special Funding Support (ZYLX201836), National Key Technology Research and Development Program of China (2018YFC2002300, 2018YFC 2002302, 2015BAI12B02), the National Natural Science Foundation of China (NSFC: 81371201) National Key Technology Research and Development Program of the Ministry of Science and Technology of The People's Republic of China (2015BAI12B04), and Hubei Province Health and Family Planning Scientific Research Project (WJ2017F057, WJ2017M208)

Background: Leukoaraiosis is characterized by white matter lesions (WMLs) on magnetic resonance imaging (MRI) and is associated with cognitive impairment. The small-world network is viewed as the optimal brain network with maximal efficiency in information processing. Patients with cognitive impairment are thought to have disrupted small-world networks. In this study, we compared the small-world network attributes between controls (study participants without memory complaints) and patients with WMLs with cognitive impairment.

Material/Methods: All study participants were prescreened using MRI and neuropsychological tests. Patients with WMLs were further divided into 2 groups according to the result of Montreal Cognitive Assessment (MoCA), i.e., WMLs with non-dementia vascular cognitive impairment (WMLs-VCIND) and WMLs with vascular dementia (WMLs-VaD). Resting-state functional MRI data were collected and applied with graph theoretical analysis to compare small-world properties between the 3 groups.

Results: We found that the overall functional connectivity strength was lowest in the WMLs-VaD patients but highest in the normal control study participants. Patients in both the WMLs-VCIND and the WMLs-VaD groups had decreased small-world properties compared with the group of normal control study participants. Moreover, the small-world properties significantly correlated with MoCA scores.

Conclusions: These findings suggest potential constructive reorganization of brain networks secondary to WMLs, and provides novel insights into the role of small-world properties in cognitive dysfunction in WMLs.

MeSH Keywords: **Leukoaraiosis • Magnetic Resonance Imaging • Mild Cognitive Impairment**

Abbreviations: **ANOVA** – analysis of variance; **ANCOVA** – analysis of covariance; **BOLD** – blood oxygenation level dependent; **CDR** – Clinical Dementia Rating scale; **FDR** – false discovery rate; **FLAIR** – fluid attenuated inversion recovery; **fMRI** – functional magnetic resonance imaging; **NC** – normal control; **MoCA** – Montreal Cognitive Assessment; **MMSE** – Mini Mental State Examination; **VCIND** – non-dementia vascular cognitive impairment; **WMLs** – white matter lesions; **VaD** – vascular dementia

Full-text PDF: https://www.medscimonit.com/abstract/index/idArt/913396

3692 7 4 63

Indexed in: [Current Contents/Clinical Medicine] [SCI Expanded] [ISI Alerting System] [ISI Journals Master List] [Index Medicus/MEDLINE] [EMBASE/Excerpta Medica] [Chemical Abstracts/CAS]

Background

Leukoaraiosis is characterized by white matter lesions (WMLs) of presumed vascular origin on T_2-weighted magnetic resonance images (MRIs) and fluid attenuated inversion recovery (FLAIR) MRIs [1]. Patients with WMLs often show increased risk of cognitive decline, especially in the attention, executive function, and information processing speed domains [2,3], and these patients consume a large amount of health resources. The onset of WMLs is insidiously destructive, and the corresponding cognitive decline is generally unnoticeable in the early stage of disease [2]; while at the same time the high prevalence of WMLs has always been considered inevitable in the elderly population [4]. Therefore, in recent years, it has become critical to determine how WMLs affect the cognitive function at an early disease stage by applying novel techniques such as function MRIs (fMRIs) or electroencephalography (EEG) in humans or animal's studies, and in most studies consistent results have been obtained [5–9]. Previous studies primarily focused on interpreting the alterations in contrast, spatial, and temporal resolution of images when applying tasked-based fMRI to decode related maps implicated in their associations. However, sometimes task completion is simply not possible, particularly for dementia patients. Recent studies have suggested that, regardless of the method of evaluation, specific cognitive functions arguably rely on distinct brain networks, such as the default mode network (DMN) and the fronto-parietal network [10,11]. Unlike task-based imaging that highlights a single brain network associated with any given task, resting state fMRI (rs-fMRI) can be simultaneously applied to multiple networks, and thus help the researchers assess the alterations in brain functional connectivity of dementia patients who simply cannot complete certain challenging tasks [12]. Therefore, rs-fMRI has been regarded as one of the most promising techniques for neuroscientists to decode brain activity, especially for elderly or patients with dementia.

The human brain has been widely considered to execute function through integrated networks, and the disruption of these networks has been reported in patients with cognitive impairment [13–15]. Both structural and functional brain networks are thought to be characterized by small-world principles regardless of either behaving or resting status [16,17]. The small-world network is a highly efficient model and is characterized by a greater local interconnectivity with short path lengths [18,19], enabling maximal efficiency in information processing at a minimal cost [20–25]. In recent years, rs-fMRI has been widely employed for the evaluation of global brain networks as well as for categorization of the disrupted small-world networks under several major conditions, including Alzheimer's disease, multiple sclerosis, traumatic brain injury, and epilepsy [26,27]. In particular, numerous studies mainly have focused on functional abnormalities in WM integrity and structural connectivity, e.g., studies on disruptions of frontal-subcortical neuronal circuits [15]. To the best of our knowledge, few studies have investigated whether dysfunction of intrinsic functional connectivity regarding global features of brain networks also occurs in WMLs patients with cognitive impairment.

This study aimed to assess the disruption of the small-world network in patients with WMLs, as well as to evaluate the correlation between the extent of alterations in small-world network and the severity of cognitive impairment, by using graph theoretical analyses [28–30] to compare the small-world properties between normal control participants without memory complaints and patients with WMLs and cognitive impairment. In addition, correlations between small-world properties and corresponding cognitive test performance were also analyzed.

Material and Methods

Ethics statement

This study was approved by the ethics committee of Beijing Tiantan Hospital, Capital Medical University, China. All participants provided written informed consents. In accordance with mandatory requirements for patients with cognitive impairment, written informed consents were obtained from their legitimate guardians.

Study participants

Initially, we recruited 53 patients with WMLs from Beijing Tiantan Hospital, Capital Medical University, China from January 2011 to January 2013. One of the patients was later excluded from data analysis because of head motion. In addition, 35 normal control (NC) study participants without memory complaints were recruited with age, gender, and education levels matching the patients. The diagnosis of WMLs was made unanimously by 2 radiologists who independently evaluated the fluid-attenuated inversion recovery (FLAIR) MRIs visually without the knowledge of the participants' clinical profiles. The rating scales was described as followed [31]: periventricular hyperintensity (PVH) was graded as 0=absence, 1="caps" or pencil-thin lining, 2=smooth "halo", and 3=irregular PVH extending into the deep white matter. Separate deep white matter hyperintense signals (DWMH) were rated as 0=absence, 1=punctate foci, 2=beginning confluence of foci, and 3=large confluent areas. The inclusion and exclusion criteria are shown in Table 1.

Clinical cognitive assessment

All study participants were instructed to complete the Chinese version of Mini Mental State Examination (MMSE) [32],

Indexed in: [Current Contents/Clinical Medicine] [SCI Expanded] [ISI Alerting System] [ISI Journals Master List] [Index Medicus/MEDLINE] [EMBASE/Excerpta Medica] [Chemical Abstracts/CAS]

Table 1. Inclusion and exclusion criteria.

Inclusion criteria	Exclusion criteria
85≥ age ≥50	Cardiac or renal failure, cancer, or other severe systemic diseases
White matter hyperintensities on FLAIR MR images	Unrelated neurological diseases
The scale of Fazekas ≥1	Chronic cerebral infarction or other lesions
Presence of a contactable informant	Leukoencephalopathy of non-vascular origin
Written informed consent	Dementia of non-vascular origin
	Psychiatric diseases or drug addiction
	Consciousness disruption or aphasia
	Inability or refusal to undergo brain MRI

the Beijing version of Montreal Cognitive Assessment (MoCA), and the Clinical Dementia Rating scale (CDR) under the supervision of a physician. The tests were completed in a strict order in accordance with standard protocols in a quiet room. The following education-specific reference cutoff values for MMSE scores were used: middle and high-27, elementary-24 and illiterate-21 [33]. Regarding to MoCA, the cutoff value for cognitive impairment was < 26 [34]. In addition, one additional point was added to the raw MoCA score when the participant's years of education were fewer than 12 years [33].

Based on the results of these cognitive tests, the study participants were divided into 3 groups: patients with non-dementia vascular cognitive impairment (WMLs-VCIND, n=32), patients with vascular dementia (WMLs-VaD, n=20), and the normal control (NC, n=35). The WMLs-VCIND patients complied with the following criteria: 1) Clinical Dementia Rating (CDR)=0.5; 2) 24≤ MMSE <27 with years of education ≥6, or 20≤ MMSE <24 with years of education years <6, or 17≤ MMSE <21 with years of education=0; and 3) MoCA <26. The WMLs-VaD patients complied with the following criteria: 1) CDR ≥1; 2) MMSE <24 with ≥6 years of education, MMSE <20 with <6 years of education, or MMSE <17 with 0 years of education; and 3) MoCA <22. The normal control group complied with the following criteria: 1) MRI showed normal brain structure; 2) CDR=0; 3) MMSE ≥27 with years of education ≥6, or MMSE ≥24 with years of education <6, or MMSE ≥21 with years of education=0; and 4) MoCA ≥26.

Brain MRI data acquisition

MRI was performed on a Siemens Magnetom Verio 3T superconducting MRI system in the Department of Radiology, Beijing Tiantan Hospital. A T_2W-FLAIR sequence was applied to detect WM hyperintensities. A standard T_1-weighted 3D magnetization prepared rapid gradient echo sequence was applied with repetition time (TR)=2300 ms, echo time (TE)=3.28 ms, time inversion (TI)=1200 ms, matrix size=256×256, flip angle (FA)=9°, slice thickness=1 mm, interslice gap=0.5 mm, and number of slices=256. Resting-state blood oxygenation level-dependent (BOLD) fMRI was performed in the axial plane using an echo-planar imaging (EPI) sequence with TR=2000 ms, TE=30 ms, FA=90°, field of view=256×256 mm^2, matrix size=64×64, NEX=1, slice thickness=3.7 mm, interslice gap=0.5 mm, number of slices=32, and acquisition time=480 seconds. A total of 240 image volumes were obtained from each study participant. Participants were instructed to stay awake, relax with their eyes closed, and remain as motionless as possible during resting fMRI scan. Rubber earplugs were used to reduce noise, and foam cushions were used to fix their head to minimize potential motion artifacts.

Rest-fMRI data preprocessing

Rest-fMRI data were preprocessed using the advanced DPARSF module of the DPABI pipeline (a toolbox for Data Processing and Analysis of Brain Imaging; *http://www.rfmri.org*) [35]. Briefly, after converting the DICOM files to NIFTI images, the first 10 time points were discarded. Then, slice timing and head motion correction were performed. One participant was excluded from the data analysis due to excessive head movement (exceeded 3.0 mm translation or 3° rotations in any direction). The data were then normalized to the standard Montreal Neurological Institute (MNI) space and re-sampled to 3-mm isotropic voxels. After smoothing with a 6 mm full width at the half maximum (FWHM) Gaussian kernel, the nuisance signals were removed. The Friston 24-parameter model was utilized to regress out head motion artefacts from the realigned data. The signals from white matter and cerebrospinal fluid were also regressed out to reduce respiratory and cardiac effects. In addition, linear and quadratic trends were included as regressors because the BOLD signal exhibits low-frequency drifts. Finally, the residual time series was band-filtered within the frequency range of 0.01–0.1 Hz to remove very low frequency drift and high frequency noise.

Indexed in: [Current Contents/Clinical Medicine] [SCI Expanded] [ISI Alerting System] [ISI Journals Master List] [Index Medicus/MEDLINE] [EMBASE/Excerpta Medica] [Chemical Abstracts/CAS]

Table 2. The demographic and clinical scores of patients in the different groups.

Variable	NC (n=35)	WMLs-VCIND (n=32)	WMLs-VaD (n=20)	F/T	*P*-value
Age, years	66.20±7.18	65.59±7.59	62.83±6.97	1.828	0.167
Woman, n (%)	17 (47.83%)	14 (45.45%)	6 (30.43%)	1.682	0.431
Education, n (%)					
Primary	0	1 (4.54%)	3 (13.04%)	1.682	0.431
Secondary	18 (52.17%)	20 (63.64%)	14 (69.56%)		
Superior	17 (47.83%)	11 (31.82%)	3 (17.40%)		
Hypertension, n(%)	13 (39.13%)	9 (27.27%)	12 (60.87%)	5.265	0.068
Smoking, n(%)	6 (17.14%)	5 (15.62%)	4 (20%)	0.514	0.773
Diabetes, n(%)	4 (11.45%)	2 (6.25%)	5 (25%)	1.364	0.505
Cholesterol, n(%)	5 (14.29%)	3 (9.37%)	6 (30%)	1.094	0.579
Body mass index	23.87±1.18	24.27±1.12	24.13±1.01	0.772	0.466
MMSE	28.91±1.31	25.54±1.84	22.04±1.99	89.89	0.000
MoCA	27.65±1.49	22.23±1.45	17.39±2.92	140.407	0.000

WMLs – white matter lesions; WMLs-VCIND – WMLs patients with non-dementia vascular cognitive impairment; WMLs-VaD – WMLs patients with vascular dementia; NC – normal controls with normal cognition; MMSE – Mini Mental State Examination; MoCA – Montreal Cognitive Assessment.

Graph theory analysis

On the processed EPI (echo planar imaging), the brain was segmented into 90 regions (45 for each hemisphere, see details in Supplementary Table 1) using an anatomical marking template according to the MNI [26,35]. Each region represented a node of the cortical network. Then, the interregional correlation coefficient matrix (R_{ij}) of the functional connectivity network was constructed as a 90×90 undirected correlation graph for each participant by calculating Pearson's correlation coefficients between the averaged time series of each possible pair of the 90 regions. A Fisher's r-to-z transform was used to increase the normality of the correlation matrix according to the following formula: $Z_r=\frac{1}{2}\ln\left(\frac{1+r}{1-r}\right)$. The r denotes the correlation coefficient between each pair, and the Z_r denote the transformed correlation. And subsequently, the graph was further converted into a binarized network based on network sparsity determination as follows:

$$A_{ij}=[a_{ij}]=\begin{cases}1 \text{ if } |a_{ij}|>T\\ 0, \text{ others}\end{cases}$$

where a_{ij} refers to the Fisher r-to-z of partial correlation coefficient from node i to node j. If the edge a_{ij} exceeds a pre-defined threshold T, it is then regarded as one; otherwise it would be set to zero. To determine the threshold T, the network sparsity (Sthr) which is defined as the ratio for the number of actual edges divided by the maximum possible number of the edges in a network, was applied to each adjacent matrix. Using the network sparsity, a patient-specific T was determined to threshold each correlation matrix so that the resulting networks have the same density level (i.e., the same number of edges) across study participants and scans [36]. The network sparsity ranging between 0.05 and 0.5, with an increment of 0.05, was reconstructed for each participant in our study. Then, all topological properties were calculated using the GRETNA software (*www.nitrc.org/projects/gretna*), and the following small-world network attributes [22] were obtained: shortest path length (Lp), clustering coefficient (Cp), global efficiency (Eg), local efficiency (Eloc), nodal efficiency (nodalE), and small-worldness parameters [37] including lambda (λ), gamma (γ), and sigma (σ), as well as the area under curve (AUC) of λ, γ, and σ with sparsity threshold as the x axis.

Statistical analysis

The chi-square test was used to evaluate the differences in gender distribution between the 3 groups. Kendall's W test was used to evaluate the difference in education years between the 3 groups. A one-way analysis of variance (ANOVA) was used to compare the differences in age; incidences of hypertension, diabetes mellitus, dyslipidemia; and histories of

Indexed in: [Current Contents/Clinical Medicine] [SCI Expanded] [ISI Alerting System] [ISI Journals Master List] [Index Medicus/MEDLINE] [EMBASE/Excerpta Medica] [Chemical Abstracts/CAS]

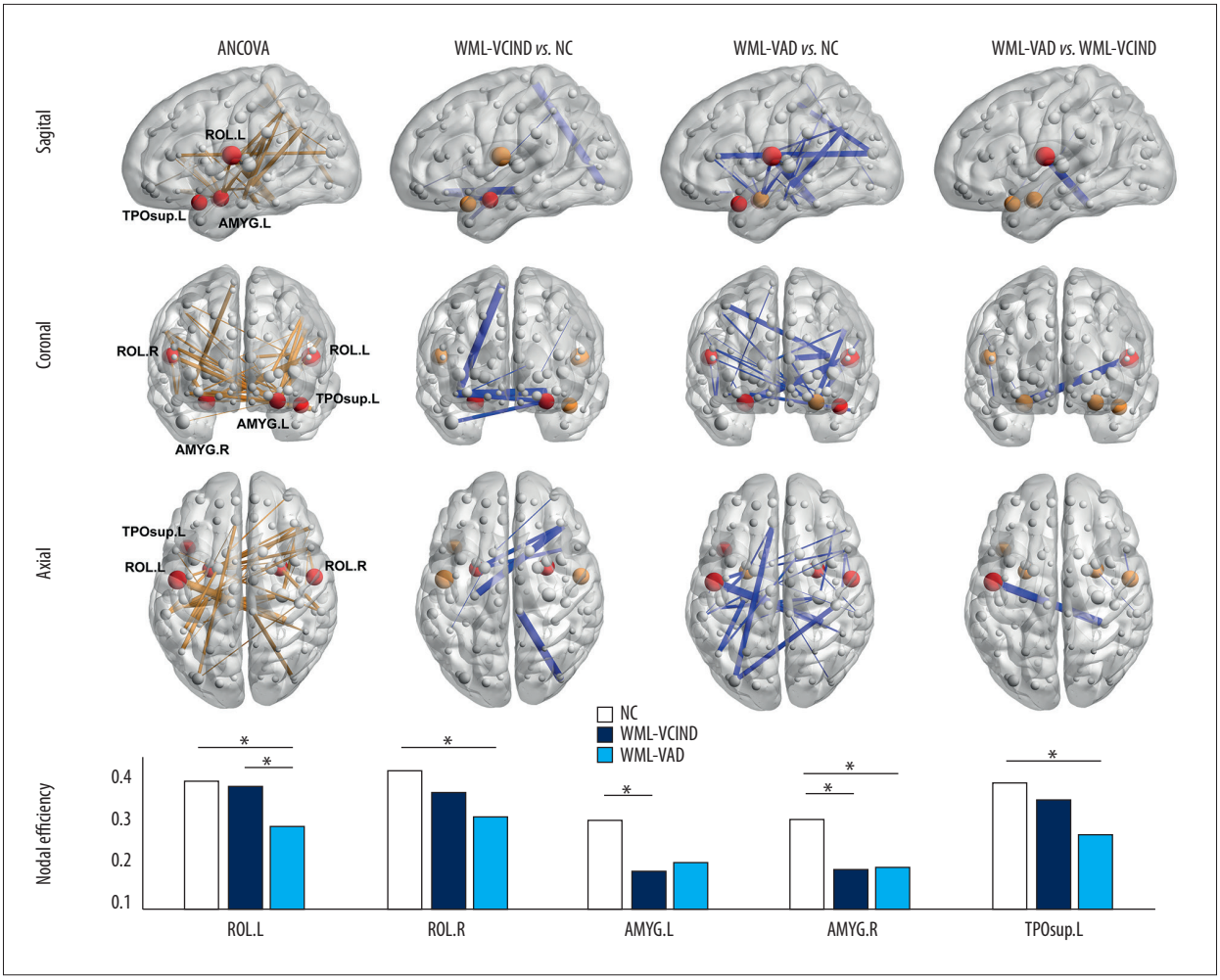

Figure 1. Group differences in regional functional connectivity (FC) and nodal efficiency (nodalE) at sparsity=0.10. Red nodes illustrated the regions with significant ANCOVA (5 nodes; *P*<0.05, FDR corrected) or Bonferroni-corrected post-hoc test results (*P*<0.05/5=0.01; also see bar graphs in the bottom panel marked with *). Lines in the figure (the top 3 panels) illustrated the FC between the connected regions were statistically different groups (yellow lines, ANCOVA test, *P*<0.001; blue lines, Bonferroni-corrected post-hoc test, *P*<0.05/39=0.00128). FDR – false discovery rate; WMLs – white matter lesions; WMLs-VCIND – WMLs patients with non-dementia vascular cognitive impairment; WMLs-VAD – WMLs patients with vascular dementia; NC – normal controls with normal cognition; nodalE – nodal efficiency; ROL.L – left rolandic operculum; ROL.R – right rolandic operculum; AMYG.L – left amygdala; AMYG.R – right amygdala; TPOsup.L – left superior temporal gyrus part.

smoking and drinking. The cognitive test results, i.e., MMSE and MoCA scores, and the brain network properties including regional functional connectivity, nodalE at sparsity=0.10, and small-worldness parameters for each sparsity level in the range of 0.05–0.5 with an increment of 0.05 were all compared using analysis of covariance (ANCOVA) using age and gender as covariances. The false discovery rate (FDR) correction was performed for the multiple comparisons of functional connectivity and nodalE values. Accordingly, *P*<0.001 was regarded as significantly different. Subsequently, Bonferroni-corrected post-hoc analysis was performed to compare the differences between the 3 groups (*P*<0.05/N, N represented the number of comparisons). Then, the Pearson's correlation analysis with FDR correction was used to evaluate the relationship between all the significantly different brain network properties and the cognitive scores within all participants, controlling for age and gender (*P*<0.05).

Results

Demographics and cognitive impairment

As shown in Table 2, No significant differences were found in age, gender, years of education, the incidences of hypertension, diabetes mellitus, dyslipidemia; or histories of smoking and

Indexed in: [Current Contents/Clinical Medicine] [SCI Expanded] [ISI Alerting System] [ISI Journals Master List] [Index Medicus/MEDLINE] [EMBASE/Excerpta Medica] [Chemical Abstracts/CAS]

Table 3. Significant group differences in FC ($P<0.001$).

ROI 1	ROI 2	zFC (mean±std)			ANCOVA		WMLs-VCIND-NC		WMLs-VAD-NC		WMLs-VAD-WMLs-VCIND	
		WMLs-VAD	WMLs-VCIND	NC	F	P	t	p	t	p	t	p
17	56	0.22±0.22	0.50±0.28	0.54±0.22	11.25	0.00	−0.58	0.56	−5.08	0.00	−3.75	0.00
38	89	0.39±0.13	0.46±0.17	0.58±0.18	9.80	0.00	−2.63	0.01	−4.03	0.00	−1.59	0.11
37	65	0.11±0.16	0.20±0.22	0.34±0.19	9.48	0.00	−2.70	0.01	−4.39	0.00	−1.48	0.14
54	70	0.43±0.26	0.47±0.22	0.69±0.25	9.35	0.00	−3.72	0.00	−3.58	0.00	−0.57	0.56
14	41	0.15±0.23	0.21±0.22	0.41±0.25	9.27	0.00	−3.31	0.00	−3.69	0.00	−0.92	0.36
39	63	0.00±0.24	0.16±0.19	0.29±0.27	9.25	0.00	−2.12	0.04	−3.80	0.00	−2.54	0.01
42	64	0.06±0.23	0.29±0.23	0.34±0.29	9.12	0.00	−0.73	0.46	−3.59	0.00	−3.42	0.00
16	38	0.33±0.14	0.35±0.26	0.54±0.21	8.96	0.00	−3.18	0.00	−3.83	0.00	−0.33	0.73
31	51	0.23±0.25	0.35±0.28	0.56±0.26	8.92	0.00	−3.12	0.00	−4.57	0.00	−1.55	0.12
61	75	0.37±0.22	0.36±0.24	0.54±0.19	8.79	0.00	−3.42	0.00	−2.90	0.00	0.23	0.81
12	41	0.12±0.24	0.18±0.27	0.39±0.27	8.77	0.00	−3.20	0.00	−3.75	0.00	−0.86	0.39
37	61	0.11±0.16	0.16±0.24	0.29±0.22	8.76	0.00	−2.25	0.03	−3.20	0.00	−0.84	0.40
41	63	0.12±0.26	0.25±0.22	0.38±0.25	8.74	0.00	−2.17	0.03	−3.56	0.00	−1.90	0.06
17	41	0.18±0.25	0.42±0.24	0.51±0.29	8.58	0.00	−1.28	0.20	−4.09	0.00	−3.34	0.00
18	84	0.47±0.28	0.74±0.26	0.78±0.31	8.53	0.00	−0.61	0.54	−3.69	0.00	−3.46	0.00
16	37	0.31±0.23	0.27±0.27	0.50±0.23	8.36	0.00	−3.70	0.00	−2.88	0.00	0.54	0.58
41	64	0.11±0.23	0.16±0.24	0.34±0.24	8.31	0.00	−3.12	0.00	−3.47	0.00	−0.72	0.47
16	41	0.33±0.21	0.29±0.23	0.51±0.26	8.27	0.00	−3.57	0.00	−2.60	0.01	0.57	0.56
12	37	0.13±0.20	0.14±0.27	0.34±0.21	8.25	0.00	−3.35	0.00	−3.62	0.00	−0.19	0.84
37	63	0.11±0.19	0.20±0.21	0.31±0.23	8.09	0.00	−2.03	0.04	−3.10	0.00	−1.41	0.16
37	62	0.07±0.15	0.05±0.27	0.23±0.18	7.99	0.00	−3.24	0.00	−3.38	0.00	0.28	0.77
38	55	0.49±0.18	0.59±0.23	0.72±0.24	7.98	0.00	−2.26	0.02	−3.58	0.00	−1.48	0.14
10	71	0.31±0.17	0.14±0.22	0.32±0.19	7.98	0.00	−3.44	0.00	−0.31	0.75	2.74	0.00
41	79	0.20±0.2	0.40±0.23	0.48±0.27	7.96	0.00	−1.27	0.20	−4.07	0.00	−3.22	0.00
80	84	0.42±0.26	0.67±0.29	0.77±0.34	7.87	0.00	−1.27	0.20	−3.87	0.00	−3.07	0.00
41	42	0.64±0.37	0.73±0.34	1.02±0.42	7.87	0.00	−3.07	0.00	−3.33	0.00	−0.89	0.37
51	58	0.39±0.28	0.51±0.31	0.70±0.23	7.84	0.00	−2.83	0.00	−4.40	0.00	−1.42	0.15
11	37	0.11±0.19	0.21±0.19	0.32±0.24	7.81	0.00	−1.97	0.05	−3.16	0.00	−1.72	0.09
41	74	0.42±0.32	0.48±0.26	0.72±0.33	7.76	0.00	−3.27	0.00	−3.22	0.00	−0.67	0.50
12	39	0.08±0.22	0.10±0.24	0.30±0.24	7.72	0.00	−3.23	0.00	−3.31	0.00	−0.38	0.70
17	81	0.96±0.26	1.19±0.26	1.23±0.28	7.66	0.00	−0.70	0.48	−3.53	0.00	−2.99	0.00
39	62	0.02±0.19	0.07±0.25	0.23±0.20	7.65	0.00	−2.81	0.00	−3.75	0.00	−0.83	0.40
31	41	0.21±0.20	0.29±0.26	0.48±0.28	7.64	0.00	−2.72	0.00	−3.75	0.00	−1.24	0.22

Indexed in: [Current Contents/Clinical Medicine] [SCI Expanded] [ISI Alerting System] [ISI Journals Master List] [Index Medicus/MEDLINE] [EMBASE/Excerpta Medica] [Chemical Abstracts/CAS]

Table 3 continued. Significant group differences in FC (P<0.001).

ROI 1	ROI 2	zFC (mean±std)			ANCOVA		WMLs-VCIND-NC		WMLs-VAD-NC		WMLs-VAD-WMLs-VCIND	
		WMLs-VAD	WMLs-VCIND	NC	F	P	t	p	t	p	t	p
42	63	0.08±0.25	0.30±0.27	0.33±0.28	7.62	0.00	–0.41	0.68	–3.27	0.00	–2.9572	0.0047
11	75	0.40±0.24	0.42±0.19	0.59±0.22	7.58	0.00	–3.27	0.00	–2.89	0.00	–0.29	0.76
16	42	0.28±0.19	0.39±0.23	0.51±0.29	7.56	0.00	–1.83	0.07	–3.19	0.00	–1.82	0.07
41	88	0.46±0.18	0.34±0.29	0.59±0.26	7.55	0.00	–3.55	0.00	–1.95	0.05	1.51	0.13
65	72	0.13±0.25	0.22±0.17	0.37±0.19	7.53	0.00	–3.27	0.00	–3.82	0.00	–1.43	0.15
14	38	0.20±0.18	0.23±0.21	0.37±0.21	7.53	0.00	–2.81	0.00	–3.10	0.00	–0.51	0.60

WMLs – white matter lesions; WMLs-VCIND – WMLs patients with non-dementia vascular cognitive impairment; WMLs-VaD – WMLs patients with vascular dementia; NC – normal controls with normal cognition; FC – functional connectivity; ROI – region of interest.

drinking between the groups. MMSE (F=46.415, P=0.000) and MoCA (F=71.962, P=0.000) were significantly different across groups with WMLs-VAD patients greater impaired compared to the other groups.

Group differences in regional functional connectivity (FC)

The ANCOVA test of the total 90*89/2=4005 regional FC pairs showed no significant differences (P<0.05, FDR corrected) among the 3 groups. While a less strict criterion (P<0.001) was used to find any possible changes, there were 39 regional FC pairs left (Figure 1, Table 3), and half of them were across 2 hemispheres. Among these 39 regional FC pairs, Bonferroni-corrected post-hoc tests were performed. These identified several regional FC pairs with significant differences between each pair of the 3 groups (P<0.05/39=0.00128). Then, we found that the rough change pattern of FC strength was WMLs-VAD < WMLs-VCIND < normal control (Figure 1, Table 3).

Group differences in global network properties

Figure 2 displays the global network properties in the 3 groups at each sparsity level in the range of 0.05–0.5 with an increment of 0.05. Statistically significant differences (ANCOVA test, P<0.05) were found among different groups, including Lp and Eg at sparsity=0.10/0.15/0.20, λ at sparsity=0.05, σ at sparsity=0.05, and AUC of Eg and Lp (Figure 2, Table 4). A Bonferroni-corrected post-hoc test showed that compared with the normal control group, both the WMLs-VCIND group and WMLs-VAD group had lower Eg and higher Lp. No significant difference was found between the WMLs-VAD group and the WMLs-VCIND group (Table 4).

Group differences in nodal efficiency (nodalE)

The nodalE values of all 90 nodes at sparsity=0.10 were compared across groups. Significant differences were found in the bilateral rolandic operculum (ROL), bilateral amygdala (AMYG), and the left temporal pole (superior temporal gyrus part) (TPOsup) across groups (P<0.05, FDR corrected) (Figure 1, Table 5). WMLs-VCIND patients showed lower nodalE in bilateral AMYG. By contrast, WMLs-VAD patients showed lower nodalE in bilateral ROL, right AMYG, and left TPOsup (P<0.01, Bonferroni corrected). Compared with WMLs-VCIND patients, WMLs-VAD patients showed lower nodalE in left ROL (P<0.01).

Relationship between small-world network properties and cognitive scores

FC between 5 pairs of brain regions (i.e., AMYG.L and bilateral supramarginal gyrus ROL.R and TPOsup.R, right inferior occipital gyrus and right paracentral lobule, and left parahippocampal gyrus to supramarginal gyrus) were significantly correlated with MoCA score in all participants combined (Figure 3, Table 6). However, there were no significant correlations between FC pairs with MMSE score (Table 6). The nodalE value of TPOsup.L significantly correlated with both MMSE (r=0.296, P=0.006) and MoCA (r=0.318, P=0.003). In addition, the nodalE of ROL.R significantly correlated with MoCA (r=0.297, P=0.006). Eg (sparsity=0.10, r=0.251, P=0.021), Lp (sparsity=0.10, r=–0.250, P=0.021), γ (sparsity=0.05, r=0.285, P=0.008), and σ (sparsity=0.05, r=0.255, P=0.018) were significantly correlated with MoCA (P<0.05) (Figure 4, Table 6). No significant correlations were found between global metrics and MMSE (Table 6).

Discussion

In the present study, we applied rs-fMRI with graph theoretical analysis to examine the small-world properties in normal control study participants, WMLs-VCIND patients, and WMLs-VAD patients. Our results revealed different patterns of functional connectivity between groups. That is, the FC strength was most

Indexed in: [Current Contents/Clinical Medicine] [SCI Expanded] [ISI Alerting System] [ISI Journals Master List] [Index Medicus/MEDLINE] [EMBASE/Excerpta Medica] [Chemical Abstracts/CAS]

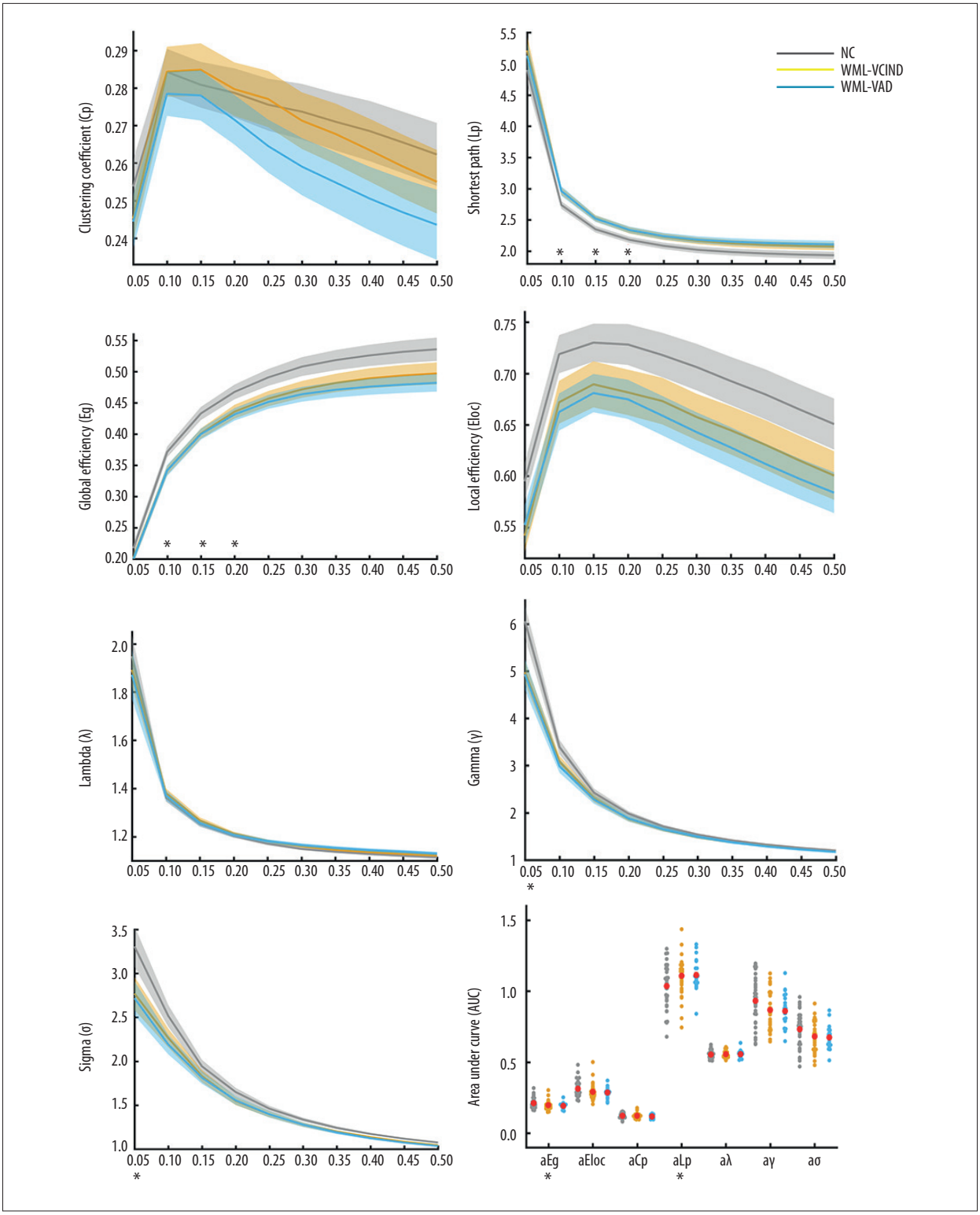

Figure 2. The global network properties in 3 groups at each sparsity level in the range of 0.05–0.5 with an increment of 0.05 and their AUC. * Marked the metrics with significant differences among groups (ANCOVA test, $P<0.05$). AUC – area under the curve.

Indexed in: [Current Contents/Clinical Medicine] [SCI Expanded] [ISI Alerting System] [ISI Journals Master List] [Index Medicus/MEDLINE] [EMBASE/Excerpta Medica] [Chemical Abstracts/CAS]

Table 4. Significant group differences in global network properties ($P<0.05$).

	Sparsity	NodalE (mean ±std)			ANCOVA		WMLs-VCIND-NC		WMLs-VaD-NC		WMLs-VaD-WMLs-VCIND	
		WMLs-VaD	WMLs-VCIND	HC	F	P	t	p	t	p	t	p
Eg	0.10	0.3417± 0.0394	0.342± 0.04	0.3715± 0.0513	4.8753	0.0100	–2.6069	0.0113	–2.2371	0.0295	–0.0208	0.9835
	0.15	0.3999± 0.0394	0.4007± 0.0466	0.433± 0.0621	4.2489	0.0175	–2.3901	0.0197	–2.1440	0.0366	–0.0626	0.9504
	0.20	0.4316± 0.0448	0.4359± 0.0627	0.4676± 0.0696	3.2255	0.0448	–1.9503	0.0555	–2.0750	0.0429	–0.2677	0.7901
	AUC	0.1928± 0.0215	0.1961± 0.0306	0.2112± 0.0359	3.1233	0.0493	–1.8430	0.0699	–2.0788	0.0425	–0.4157	0.6794
Lp	0.10	2.9634± 0.3439	2.9623± 0.34	2.7396± 0.3594	4.5685	0.0131	2.5992	0.0116	2.2560	0.0282	0.0115	0.9909
	0.15	2.5218± 0.2323	2.5267± 0.2807	2.3518± 0.3084	4.0443	0.0211	2.4194	0.0184	2.1395	0.0370	–0.0648	0.9486
	0.20	2.34± 0.2356	2.3342± 0.2941	2.1814± 0.298	3.2915	0.0422	2.1103	0.0387	2.0419	0.0461	0.0747	0.9407
	AUC	1.1133± 0.1145	1.1088± 0.1494	1.0346± 0.154	3.1208	0.0494	1.9989	0.0498	1.9898	0.0518	0.1147	0.9091
γ	0.05	4.93± 1.4788	4.9776± 1.3555	6.0564± 2.0495	4.0224	0.0216	–2.5157	0.0144	–2.1545	0.0358	–0.1191	0.9057
σ	0.05	2.7178± 0.8709	2.7719± 1.0742	3.3076± 1.372	4.1130	0.0199	–1.7677	0.0818	–1.7298	0.0895	–0.1894	0.8505

WMLs – white matter lesions; WMLs-VCIND – WMLs patients with non-dementia vascular cognitive impairment; WMLs-VaD – WMLs patients with vascular dementia; NC – normal controls with normal cognition; Eg – global efficiency; Lp – shortest path length; γ – gamma; σ – sigma; ANCOVA – analysis of covariance.

Table 5. Significant group differences in nodal efficiency (NodalE; $P<0.05$, FDR corrected).

No.	Region	NodalE (mean ±std)			ANCOVA		WMLs-VCIND-NC		WMLs-VaD-NC		WMLs-VaD-WMLs-VCIND	
		NC	WMLs-VCIND	WMLs-VaD	F	P	t	p	t	p	t	p
17	ROL.L	0.4056± 0.0981	0.3888± 0.0915	0.2952± 0.1187	8.2297	0.0006	–0.7222	0.4727	–3.7176	0.0005	–3.1990	0.0024
18	ROL.R	0.4253± 0.1046	0.3765± 0.1138	0.3178± 0.078	7.0066	0.0016	–1.8274	0.0722	–3.9960	0.0002	–2.0248	0.0482
41	AMYG.L	0.3112± 0.1458	0.1906± 0.1706	0.2122± 0.1333	6.4868	0.0024	–3.1193	0.0027	–2.4980	0.0156	0.4813	0.6324
42	AMYG.R	0.3136± 0.1438	0.1937± 0.1724	0.2011± 0.1454	7.1397	0.0014	–3.0998	0.0029	–2.7789	0.0075	0.1589	0.8744
83	TPOsup.L	0.3997± 0.1197	0.3582± 0.1286	0.2747± 0.1516	6.4221	0.0026	–1.3653	0.1769	–3.3768	0.0014	–2.1278	0.0383

WMLs – white matter lesions; WMLs-VCIND – WMLs patients with non-dementia vascular cognitive impairment; WMLs-VaD – WMLs patients with vascular dementia; NC – normal controls with normal cognition; nodalE – nodal efficiency; ROL.L – left rolandic operculum; ROL.R – right rolandic operculum; AMYG.L – left amygdala; AMYG.R – right amygdala; TPOsup.L – left superior temporal gyrus part; ANCOVA – analysis of covariance.

Indexed in: [Current Contents/Clinical Medicine] [SCI Expanded] [ISI Alerting System] [ISI Journals Master List] [Index Medicus/MEDLINE] [EMBASE/Excerpta Medica] [Chemical Abstracts/CAS]

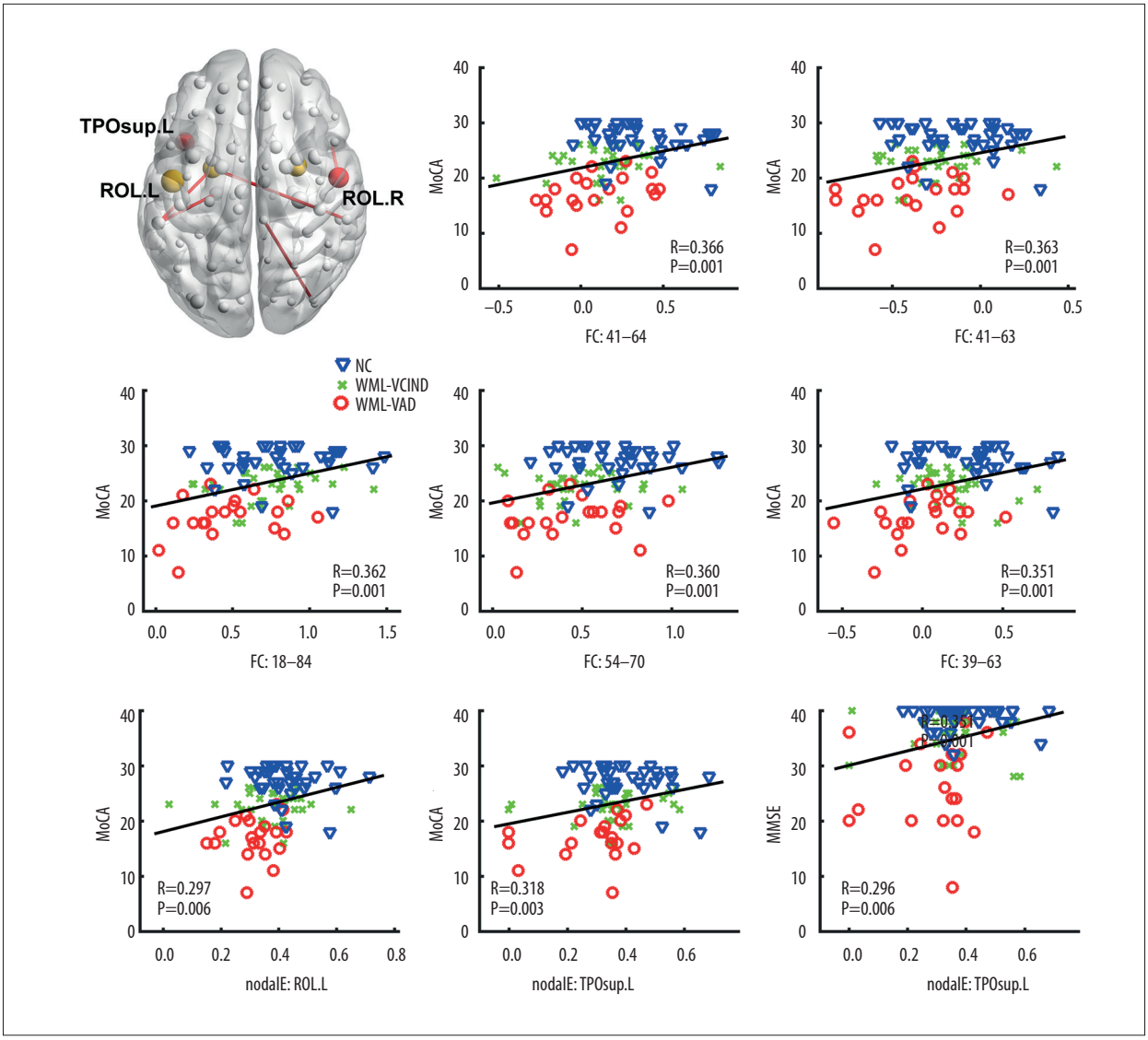

Figure 3. Significant correlations between brain network properties (regional functional connectivity and nodal efficiency (nodalE)) and cognitive performance (MMSE and MoCA scores). WMLs – white matter lesions; WMLs-VCIND – WMLs patients with non-dementia vascular cognitive impairment; WMLs-VAD – WMLs patients with vascular dementia; NC – normal controls with normal cognition; nodalE – nodal efficiency; ROL.L – left rolandic operculum; ROL.R – right rolandic operculum; TPOsup.L – left superior temporal gyrus part; MMSE – Mini Mental State Examination; MoCA – Montreal Cognitive Assessment.

impaired in the WMLs-VAD group compared to the other groups. In addition, patient groups showed disturbed small-world networks (lower Eg and higher Lp), compared to the normal control study participants. In nodalE, functional connectivity networks showed altered nodal characteristic in both cortical and subcortial regions, such as the bilateral rolandic operculum (ROL), bilateral amygdala (AMYG), and the left temporal pole (superior temporal gyrus part) (TPOsup). Finally, significant correlations were found between small-world network properties and cognition in WMLs patients.

Altered global network properties

Consistent with previous studies [38,39], our study showed that small-world network properties were conserved in WMLs patients with cognitive impairment. The human brain is viewed as a complex but efficient neural network to maximize the power of information processing for the large clustering coefficients but short characteristic path lengths [40,41]. Such a topology has been related to normal human cognitive functioning [16,42–46]. However, in this study, WMLs patients with different levels of cognitive impairment all showed longer characteristic path lengths and lower global efficiency over a wide

Indexed in: [Current Contents/Clinical Medicine] [SCI Expanded] [ISI Alerting System] [ISI Journals Master List] [Index Medicus/MEDLINE] [EMBASE/Excerpta Medica] [Chemical Abstracts/CAS]

Table 6. Relationship between brain network properties and behaviors.

	MMSE		MoCA	
	R	*P*	R	*P*
Global metrics (*P*<0.05)				
Eg_0.10	.117	.287	.251	.021
Eg_0.15	.108	.325	.192	.078
Eg_0.20	.064	.562	.156	.153
Eg_AUC	.066	.547	.166	.130
Lp_0.10	–.095	.386	–.250	.021
Lp_0.15	–.094	.392	–.190	.082
Lp_0.20	–.061	.579	–.155	.157
Lp_AUC	–.064	.563	–.172	.116
Gamma_0.05	.208	.056	.285	.008
Sigma_0.05	.207	.057	.255	.018
NodalE (Bonferroni *P*<0.05/5=0.01)				
ROL.L	.187	.087	.270	.012
ROL.R	.177	.105	.297	.006
AMYG.L	.241	.026	.270	.012
AMYG.R	.180	.100	.205	.060
TPOsup.L	.296	.006	.318	.003
FC (Bonferroni *P*<0.05/39=0.00128)				
FC_41-64	.273	.011	.366	.001
FC_41-63	.265	.014	.363	.001
FC_18-84	.295	.006	.362	.001
FC_54-70	.262	.015	.360	.001
FC_39-63	.293	.007	.351	.001

MMSE – Mini Mental State Examination; MoCA – Montreal Cognitive Assessment; Eg – global efficiency; AUC – area under the curve; Lp – shortest path length; nodalE – nodal efficiency; ROL.L – left rolandic operculum; ROL.R – right rolandic operculum; AMYG.L – left amygdala; AMYG.R – right amygdala; TPOsup.L – left superior temporal gyrus part; FC – functional connectivity.

range of sparsity than normal control study participants. This study finding provides further evidence that WMLs patients with cognitive impairment have an altered small-worldness (Figure 2) and suggests that the neural architecture of WMLs patients with cognitive impairment might be less optimized than normal control study participants.

Functional connectivity defines the temporal correlation between functional measurements between different areas [47]. In this study, the functional connectivity strength was significantly lower in patients with WMLs than normal control study participants, which means the extent of local connectedness decreased in WMLs patients. In addition, compared with normal control study participants, WMLs patients had longer Lp. The Lp is considered a measure of the global capacity for parallel information integration between different cortical regions [40,42]. Information interactions between interconnected brain regions are believed to be a basis of the human cognitive process [28,48,49]. The longer Lp in WMLs patients might suggest that information processing between distant brain regions is disrupted, providing additional evidence for mechanisms of cognitive impairment. Compared with normal control study participants, WMLs patients showed a significant decrease in global efficiency (Eg). Eg is an index for the overall capacity or efficiency of the parallel information transfer and integrated processing in the network. Our results suggest that the Eg decrease might be a marker of brain functional plasticity [50,51].

Altered nodal network properties

The nodal efficiency (nodalE) is an index for reflecting the roles of nodes in information processing [50,52]. The present study

Indexed in: [Current Contents/Clinical Medicine] [SCI Expanded] [ISI Alerting System] [ISI Journals Master List] [Index Medicus/MEDLINE] [EMBASE/Excerpta Medica] [Chemical Abstracts/CAS]

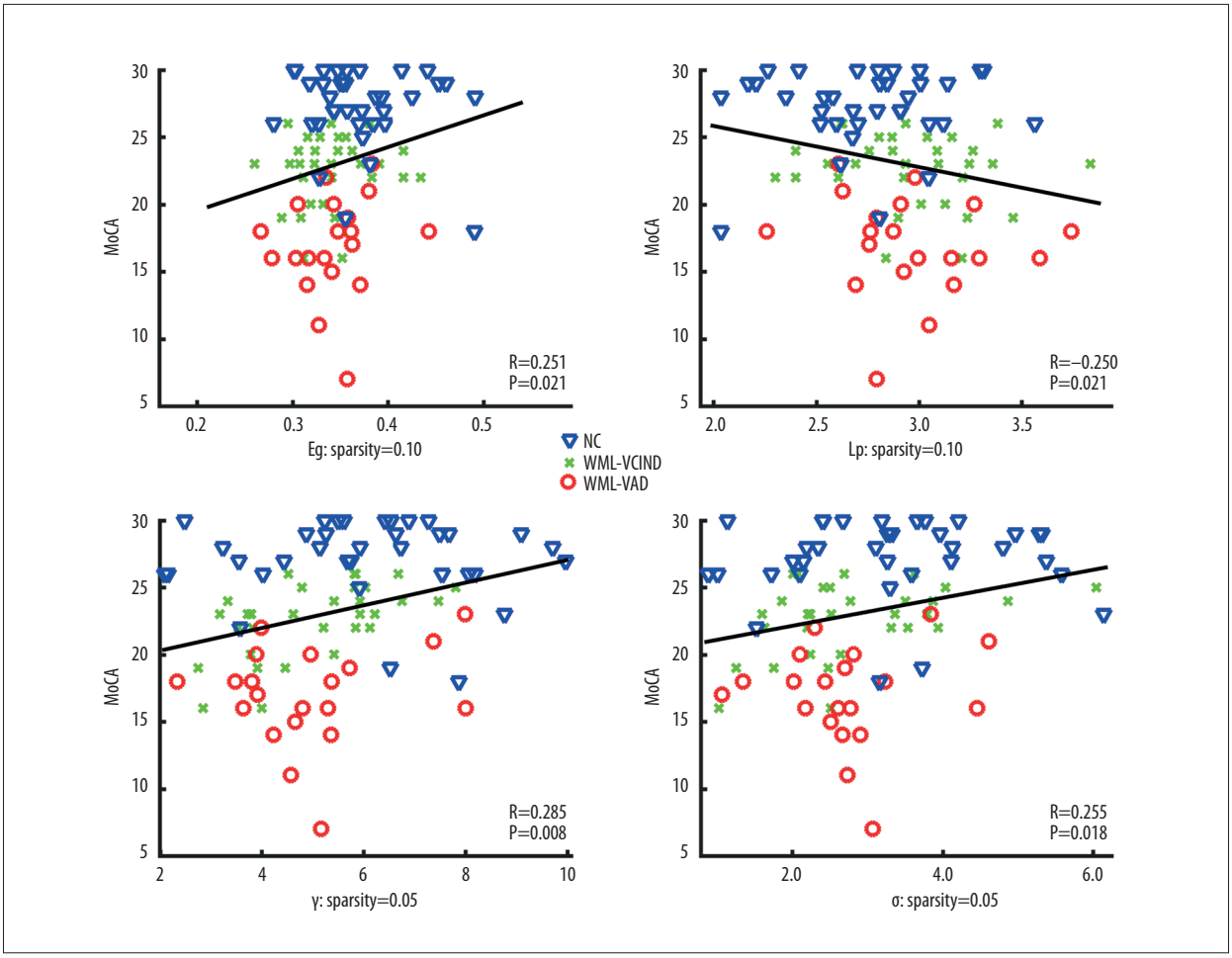

Figure 4. Significant correlations between brain network properties (global metrics) and cognitive performance (MoCA scores). WMLs – white matter lesions; WMLs-VCIND – WMLs patients with non-dementia vascular cognitive impairment; WMLs-VAD: WMLs patients with vascular dementia; NC – normal controls with normal cognition; shortest path length (Lp), global efficiency (Eg), gamma (γ) and sigma (σ); MoCA – Montreal Cognitive Assessment.

showed that compared with normal control study participants, WMLs-VCIND patients and WMLs-VaD patients had altered nodal characteristic in the cortical and subcortical regions.

We observed the amygdala presented a nodalE decrease in WMLs-VCIND patients, although these alterations were not correlated with cognitive scores. Abnormal amygdala activity is believed to be associated with decreased social intelligence and other related symptoms, such as difficulty in memory [53]. The amygdala may be an important hub that participates in the pathological process of cognitive impairment. The decreased functional connectivity from the amygdala to other brain regions might reflect a disruption in a "relevance detection network" which affects the processing of stimuli that are relevant for the organism's self-regulating functions [54]. More behavioral and neuroimaging studies should be conducted to test this hypothesis.

Unexpectedly, we found that the altered nodes of regional functional connectivity in WMLs-VaD patients were asymmetrically distributed. The right amygdala and the left temporal pole regions showed a decrease in nodalE. Furthermore, these alterations were correlated with the cognitive scores. The amygdala is considered a part of the default mode network [55,56]. The abnormal default mode network function might underlie the pathophysiological mechanism of cognitive impairment [50,51,57]. The present results reconfirm the amygdala as one of the hub nodes in the brain's default network. The WMLs-VaD patients had lower nodalE in the bilateral ROL, which are implicated in the semantic processing of language [58,59]. Of note, the alterations were correlated with the MoCA score. These results may suggest that the ROL is a hub brain node for processing cognition.

Indexed in: [Current Contents/Clinical Medicine] [SCI Expanded] [ISI Alerting System] [ISI Journals Master List] [Index Medicus/MEDLINE] [EMBASE/Excerpta Medica] [Chemical Abstracts/CAS]

Relationship between topological measurements and cognitive behaviors

Importantly, the clinical cognitive scores were correlated with small-world network topological properties (FC, nodalE, Eg, Lp, λ, σ). A severe cognitive impairment has been widely regarded as being correlated with a number of factors, including lower degree of connectivity, lower global and local efficiency, and a longer absolute path length and decreased small-worldness [22]. These findings indicate that the altered small-world properties can serve as sensitive imaging markers for cognitive impairment in WMLs patients.

Decreased small-worldness in aged participants is thought to be caused by a reduction in the sensitivity of the neurons undergoing the stimuli [42]. In addition, WMLs can negatively affect the optimal balance between information transmission and functional integration [60]. Therefore, decreased small-worldness in WMLs patients in this study might suggest an interruption of local specialization due to white matter damage. This is compatible with the theory that small-world topology appears when networks are evolved for an optimal balance between local specialization and global integration [61]. Because the small-world network model reflects an optimal balance between local specialization and global integration, our findings and the aforementioned literature together indicate constructive reorganization, though less optimal, of brain networks secondary to WMLs [62]. Because cortical information integration is the fundamental basis of human cognitive processes [40], our results provide new insights into the association between alternations in human brain small-world properties and cognitive dysfunction associated with WMLs.

The MoCA score is an established biomarker for cognitive impairment. The results of this study showed that the small-world properties correlated with the MoCA score but not the MMSE score. This finding was consistent with a previous finding that the MMSE score is insensitive to mild cognitive impairment [63].

Limitations

Despite these promising findings, there were limitations to our study. In additional to functional brain networks, future research is warranted to clarify structural brain networks with diffusion tensor imaging to establish an integrated view of structural and functional brain network changes and their associations with cognition in WMLs. Despite the fact that we cannot make direct connections between different levels of cognitive impairment and global features of the brain network, possibly due to the small sample properties, future studies exploring the differences pertaining to the distinctive features of the small-world network with a larger cohort of patients, WMLs-VCIND and WMLs-VAD patients in particular, based on their clinical stratification or even different scaling of cognitive dysfunction, should be further carried out.

Conclusions

The present study comprehensively compared the small-world topological properties in WMLs patients with cognitive impairment with those in normal control study participants. Our results are in line with the concept that the brain is an economical small-world functional network. Specifically, we found that WMLs patients had altered small-world properties as characterized by low local and global efficiency at a relatively low wiring cost, suggesting constructive reconstruction following white matter damage. The lower global and nodal efficiency of WMLs patients suggest a loss of economic organization of the brain's functional network. Importantly, the network efficiency is significantly negatively correlated with the level of cognitive impairment, which leads us to believe that the changes in the small-world network topological characteristics might provide new insights into the pathophysiology of cognitive impairment in WMLs. The graph theoretical analysis of small-world properties can potentially be used to evaluate the progression of cognitive impairment in WMLs patients.

Conflict of interest

None.

Indexed in: [Current Contents/Clinical Medicine] [SCI Expanded] [ISI Alerting System] [ISI Journals Master List] [Index Medicus/MEDLINE] [EMBASE/Excerpta Medica] [Chemical Abstracts/CAS]

Supplementary Table

Supplementary Table 1. Cortical and sub-cortical regions defined in automated anatomical labeling template image.

1	Precentral_L	31	Cingulum_Ant_L	61	Parietal_Inf_L
2	Precentral_R	32	Cingulum_Ant_R	62	Parietal_Inf_L
3	Frontal_Sup_L	33	Cingulum_Mid_L	63	SupraMarginal_L
4	Frontal_Sup_R	34	Cingulum_Mid_R	64	SupraMarginal_R
5	Frontal_Sup_Orb_L	35	Cingulum_Post_L	65	Angular_L
6	Frontal_Sup_Orb_R	36	Cingulum_Post_R	66	Angular_R
7	Frontal_Mid_L	37	Hippocampus_L	67	Precuneus_L
8	Frontal_Mid_R	38	Hippocampus_R	68	Precuneus_R
9	Frontal_Mid_ Orb_L	39	ParaHippocampal_L	69	Paracentral_Lobule_L
10	Frontal_Mid_ Orb_R	40	ParaHippocampal_R	70	Paracentral_Lobule_R
11	Frontal_Inf_Oper_L	41	Amygdala_L	71	Caudate_L
12	Frontal_Inf_Oper_R	42	Amygdala_R	72	Caudate_R
13	Frontal_Inf_Tri_L	43	Calcarine_L	73	Putamen_L
14	Frontal_Inf_Tri_R	44	Calcarine_R	74	Putamen_R
15	Frontal_Inf_ Orb_L	45	Cuneus_L	75	Pallidum_L
16	Frontal_Inf_ Orb_R	46	Cuneus_R	76	Pallidum_R
17	Rolandic_Oper_L	47	Lingual_L	77	Thalamus_L
18	Rolandic_Oper_R	48	Lingual_R	78	Thalamus_R
19	Supp_Motor_Area_L	49	Occipital_Sup_L	79	Heschl_L
20	Supp_Motor_Area_R	50	Occipital_Sup_R	80	Heschl_R
21	Olfactory_L	51	Occipital_Mid_L	81	Temporal_Sup_L
22	Olfactory_R	52	Occipital_Mid_R	82	Temporal_Sup_R
23	Frontal_Sup_Medial_L	53	Occipital_Inf_L	83	Temporal_Pole_Sup_L
24	Frontal_Sup_Medial_R	54	Occipital_Inf_R	84	Temporal_Pole_Sup_R
25	Frontal_Mid_ Orb_L	55	Fusiform_L	85	Temporal_Mid_L
26	Frontal_Mid_ Orb_R	56	Fusiform_R	86	Temporal_Mid_R
27	Rectus_L	57	Postcentral_L	87	Temporal_Pole_Mid_L
28	Rectus_R	58	Postcentral_R	88	Temporal_Pole_Mid_R
29	Insula_L	59	Parietal_Sup_L	89	Temporal_Inf_L
30	Insula_R	60	Parietal_Sup_R	90	Temporal_Inf_R

Indexed in: [Current Contents/Clinical Medicine] [SCI Expanded] [ISI Alerting System] [ISI Journals Master List] [Index Medicus/MEDLINE] [EMBASE/Excerpta Medica] [Chemical Abstracts/CAS]

References:

1. Steingart A, Hachinski VC, Lau C et al: Cognitive and neurologic findings in subjects with diffuse white matter lucencies on computed tomographic scan (leuko-araiosis). Arch Neurol, 1987; 44: 32–35
2. Debette S, Markus HS: The clinical importance of white matter hyperintensities on brain magnetic resonance imaging: Systematic review and meta-analysis. BMJ, 2010; 341: c3666
3. Verdelho A, Madureira S, Moleiro C et al: White matter changes and diabetes predict cognitive decline in the elderly: the LADIS study. Neurology, 2010; 75: 160–67
4. Zhou G, Ren S, Chen N et al: Cerebral white matter lesions and cognitive function in a non-demented Chinese veteran cohort. J Int Med Res, 2008; 36: 115–22
5. Menon V, Ford JM, Lim KO et al: Combined event-related fMRI and EEG evidence for temporal-parietal cortex activation during target detection. Neuroreport, 1997; 8: 3029–37
6. Krakow K, Allen PJ, Symms MR et al: EEG recording during fMRI experiments: Image quality. Hum Brain Mapp, 2000; 10: 10–15
7. Krakow K, Woermann FG, Symms MR et al: EEG-triggered functional MRI of interictal epileptiform activity in patients with partial seizures. Brain, 1999; 122(Pt 9): 1679–88
8. Bonmassar G, Anami K, Ives J et al: Visual evoked potential (VEP) measured by simultaneous 64-channel EEG and 3T fMRI. Neuroreport, 1999; 10: 1893–97
9. Hess A, Stiller D, Kaulisch T et al: New insights into the hemodynamic blood oxygenation level-dependent response through combination of functional magnetic resonance imaging and optical recording in gerbil barrel cortex. J Neurosci, 2000; 20: 3328–38
10. Greicius MD, Srivastava G, Reiss AL et al: Default-mode network activity distinguishes Alzheimer's disease from healthy aging: Evidence from functional MRI. Proc Natl Acad Sci USA, 2004; 101: 4637–42
11. Bressler SL, Menon V: Large-scale brain networks in cognition: Emerging methods and principles. Trends Cogn Sci, 2010; 14: 277–90
12. Shen HH: Core concept: Resting-state connectivity. Proc Natl Acad Sci USA, 2015; 112: 14115–16
13. Douw L, van Dellen E, Baayen JC et al: The lesioned brain: Still a small-world? Front Hum Neurosci, 2010; 4: 174
14. Rubinov M, Sporns O: Complex network measures of brain connectivity: Uses and interpretations. Neuroimage, 2010; 52: 1059–69
15. Andrade SP, Brucki SM, Bueno OF et al: Neuropsychological performance in patients with subcortical stroke. Arq Neuropsiquiatr, 2012; 70: 341–47
16. Watts DJ, Strogatz SH: Collective dynamics of 'small-world' networks. Nature, 1998; 393: 440–42
17. Humphries MD, Gurney K, Prescott TJ: The brainstem reticular formation is a small-world, not scale-free, network. Proc Biol Sci, 2006; 273: 503–11
18. He Y, Chen ZJ, Evans AC: Small-world anatomical networks in the human brain revealed by cortical thickness from MRI. Cereb Cortex, 2007; 17: 2407–19
19. Bullmore ET, Bassett DS: Brain graphs: Graphical models of the human brain connectome. Annu Rev Clin Psychol, 2011; 7: 113–40
20. Bosma I, Douw L, Bartolomei F et al: Synchronized brain activity and neurocognitive function in patients with low-grade glioma: A magnetoencephalography study. Neuro Oncol, 2008; 10: 734–44
21. Douw L, Baayen H, Bosma I et al: Treatment-related changes in functional connectivity in brain tumor patients: A magnetoencephalography study. Exp Neurol, 2008; 212: 285–90
22. Liu Y, Liang M, Zhou Y et al: Disrupted small-world networks in schizophrenia. Brain, 2008; 131: 945–61
23. Stephan KE, Riera JJ, Deco G et al: The Brain Connectivity Workshops: Moving the frontiers of computational systems neuroscience. Neuroimage, 2008; 42: 1–9
24. Bosma I, Reijneveld JC, Klein M et al: Disturbed functional brain networks and neurocognitive function in low-grade glioma patients: A graph theoretical analysis of resting-state MEG. Nonlinear Biomed Phys, 2009; 3: 9
25. Wang Q, Su TP, Zhou Y et al: Anatomical insights into disrupted small-world networks in schizophrenia. Neuroimage, 2012; 59: 1085–93
26. Stam CJ: Modern network science of neurological disorders. Nat Rev Neurosci, 2014; 15: 683–95
27. Yang Y, Tao L, Qian Z et al: [Study on the brain network characteristics before and after the operation of frontotemporal tumor patients.] Chinese Journal of Biomedical Engineering, 2018; 2 [in Chinese]
28. Stam CJ, Reijneveld JC: Graph theoretical analysis of complex networks in the brain. Nonlinear Biomed Phys, 2007; 1: 3
29. Bullmore E, Sporns O: Complex brain networks: Graph theoretical analysis of structural and functional systems. Nat Rev Neurosci, 2009; 10: 186–98
30. Micheloyannis S, Vourkas M, Tsirka V et al: The influence of ageing on complex brain networks: A graph theoretical analysis. Hum Brain Mapp, 2009; 30: 200–8
31. Fazekas F, Chawluk JB, Alavi A et al: MR signal abnormalities at 1.5 T in Alzheimer's dementia and normal aging. Am J Roentgenol, 1987; 149: 351–56
32. Katzman R, Zhang MY, Ouang Ya Q et al: A Chinese version of the Mini-Mental State Examination; Impact of illiteracy in a Shanghai dementia survey. J Clin Epidemiol, 1988; 41: 971–78
33. Nasreddine ZS, Phillips NA, Bedirian V et al: The Montreal Cognitive Assessment, MoCA: A brief screening tool for mild cognitive impairment. J Am Geriatr Soc, 2005; 53: 695–99
34. Crum RM, Anthony JC, Bassett SS et al: Population-based norms for the Mini-Mental State Examination by age and educational level. JAMA, 1993; 269: 2386–91
35. Yan CG, Wang XD, Zuo XN et al: DPABI: Data processing and analysis for (resting-state) brain imaging. Neuroinformatics, 2016; 14: 339–51
36. Qian S, Sun G, Jiang Q et al: Altered topological patterns of large-scale brain functional networks during passive hyperthermia. Brain Cogn, 2013; 83: 121–31
37. Liu Y, Duan Y, He Y et al: Altered topological organization of white matter structural networks in patients with neuromyelitis optica. PLoS One, 2012; 7: e48846
38. Yu Y, Zhou X, Wang H et al: Small-world brain network and dynamic functional distribution in patients with subcortical vascular cognitive impairment. PLoS One, 2015; 10: e0131893
39. Faskhodi MM, Einalou Z, Dadgostar M: Diagnosis of Alzheimer's disease using resting-state fMRI and graph theory. Technol Health Care, 2018; 26(6): 921–31
40. Sporns O, Zwi JD: The small world of the cerebral cortex. Neuroinformatics, 2004; 2: 145–62
41. Kaiser M, Hilgetag CC: Nonoptimal component placement, but short processing paths, due to long-distance projections in neural systems. PLoS Comput Biol, 2006; 2: e95
42. Achard S, Bullmore E: Efficiency and cost of economical brain functional networks. PLoS Comput Biol, 2007; 3: e17
43. He Y, Dagher A, Chen Z et al: Impaired small-world efficiency in structural cortical networks in multiple sclerosis associated with white matter lesion load. Brain, 2009; 132: 3366–79
44. Wang L, Zhu C, He Y et al: Altered small-world brain functional networks in children with attention-deficit/hyperactivity disorder. Hum Brain Mapp, 2009; 30: 638–49
45. Zhao X, Liu Y, Wang X et al: Disrupted small-world brain networks in moderate Alzheimer's disease: A resting-state FMRI study. PLoS One, 2012; 7: e33540
46. Feng Y, Bai L, Ren Y et al: Investigation of the large-scale functional brain networks modulated by acupuncture. Magn Reson Imaging, 2011; 29: 958–65
47. Friston KJ, Frith CD, Liddle PF et al: Functional connectivity: The principal-component analysis of large (PET) data sets. J Cereb Blood Flow Metab, 1993; 13: 5–14
48. Tononi G, Edelman GM, Sporns O: Complexity and coherency: Integrating information in the brain. Trends Cogn Sci, 1998; 2: 474–84
49. Horwitz B: The elusive concept of brain connectivity. Neuroimage, 2003; 19: 466–70
50. Song M, Du H, Wu N et al: Impaired resting-state functional integrations within default mode network of generalized tonic-clonic seizures epilepsy. PLoS One, 2011; 6: e17294
51. Wang Z, Lu G, Zhang Z et al: Altered resting state networks in epileptic patients with generalized tonic-clonic seizures. Brain Res, 2011; 1374: 134–41

Indexed in: [Current Contents/Clinical Medicine] [SCI Expanded] [ISI Alerting System] [ISI Journals Master List] [Index Medicus/MEDLINE] [EMBASE/Excerpta Medica] [Chemical Abstracts/CAS]

52. Hagmann P, Cammoun L, Gigandet X et al: Mapping the structural core of human cerebral cortex. PLoS Biol, 2008; 6: e159
53. Zalla T, Sperduti M: The amygdala and the relevance detection theory of autism: An evolutionary perspective. Front Hum Neurosci, 2013; 7: 894
54. Baron-Cohen S, Ring HA, Bullmore ET et al: The amygdala theory of autism. Neurosci Biobehav Rev, 2000; 24: 355–64
55. Raichle ME: Cognitive neuroscience. Bold insights. Nature, 2001; 412: 128–30
56. Fransson P: Spontaneous low-frequency BOLD signal fluctuations: An fMRI investigation of the resting-state default mode of brain function hypothesis. Hum Brain Mapp, 2005; 26: 15–29
57. Luo C, Li Q, Lai Y et al: Altered functional connectivity in default mode network in absence epilepsy: A resting-state fMRI study. Hum Brain Mapp, 2011; 32: 438–49
58. Demb JB, Desmond JE, Wagner AD et al: Semantic encoding and retrieval in the left inferior prefrontal cortex: A functional MRI study of task difficulty and process specificity. J Neurosci, 1995; 15: 5870–78
59. Behroozmand R, Shebek R, Hansen DR et al: Sensory-motor networks involved in speech production and motor control: An fMRI study. Neuroimage, 2015; 109: 418–28
60. Vallet GT, Hudon C, Simard M et al: The disconnection syndrome in the Alzheimer's disease: The cross-modal priming example. Cortex, 2013; 49: 2402–15
61. Chen ZJ, He Y, Rosa-Neto P et al: Revealing modular architecture of human brain structural networks by using cortical thickness from MRI. Cereb Cortex, 2008; 18: 2374–81
62. Latora V, Marchiori M: Efficient behavior of small-world networks. Phys Rev Lett, 2001; 87: 198701
63. Tombaugh TN, McIntyre NJ: The mini-mental state examination: A comprehensive review. J Am Geriatr Soc, 1992; 40: 922–35

Indexed in: [Current Contents/Clinical Medicine] [SCI Expanded] [ISI Alerting System] [ISI Journals Master List] [Index Medicus/MEDLINE] [EMBASE/Excerpta Medica] [Chemical Abstracts/CAS]